

1 National and regional seasonal dynamics of all-cause and cause-specific mortality in the  
2 USA from 1980 to 2013<sup>36</sup>  
3 Robbie M Parks<sup>1,2</sup>, James E Bennett<sup>1,2,3</sup>, Kyle J Foreman<sup>1,2,4</sup>, Ralf Toumi<sup>5</sup>, Majid Ezzati<sup>1,2,3\*</sup>  
4 <sup>1</sup> MRC-PHE Centre for Environment and Health, Imperial College London, London, United  
5 Kingdom, W2 1PG  
6 <sup>2</sup> Department of Epidemiology and Biostatistics, School of Public Health, Imperial College  
7 London, London, United Kingdom, W2 1PG  
8 <sup>3</sup> WHO Collaborating Centre on NCD Surveillance and Epidemiology, Imperial College  
9 London, London, United Kingdom, W2 1PG  
10 <sup>4</sup> Institute for Health Metrics and Evaluation, University of Washington, Seattle, USA, WA  
11 98121  
12 <sup>5</sup> Space and Atmospheric Physics, Imperial College London, London, United Kingdom, W7  
13 2AZ  
14 Address correspondence to Majid Ezzati (majid.ezzati@imperial.ac.uk)

- Style Definition: Normal: Font:(Default) Times New Roman, 12 pt, Space After: 0 pt, Line spacing: single
- Style Definition: EndNote Bibliography
- Style Definition: Comment Text
- Style Definition: Footer
- Style Definition: Caption
- Style Definition: Balloon Text
- Style Definition: EndNote Bibliography Title
- Style Definition: List Paragraph
- Style Definition: Header

Formatted: Left, Line spacing: single

## 16 Abstract

17 It has been hypothesized that a warmer world may lower winter mortality in temperate  
18 climates, where winter deaths exceed summer ones. However, there is limited information on  
19 how the timing and the relative magnitudes of minimum and maximum mortality, by local  
20 climate age group, sex and medical cause of death. We used geo-coded mortality data and  
21 wavelet analytical techniques wavelets to analyse the seasonality of all-cause and cause-specific  
22 mortality by age group and sex from 1980 to 20136 in the USA, nationally and in its subnational  
23 climatic regions. Death rates in men and women  $\geq 45$  years exhibited statistically significant  
24 seasonality with peak in January/peaked in December to February and minimum were lowest  
25 in June/July to August, driven by seasonality of cardiorespiratory diseases and injuries. In these  
26 ages, percent difference in death rates between peak and minimum months did not vary across  
27 climate regions, and was largely unchanged nor changed from 1980 to 20136. Under five years  
28 of age, seasonality of all-cause mortality largely disappeared after the 1990s. In adolescents  
29 and young adults, especially in males, death rates peaked in June/July and were lowest in  
30 December/January, driven by seasonality of injury deaths.

31

## 32 Introduction

33 It is well-established that death rates vary throughout the year, and in temperate climates there  
34 tend to be more deaths in winter than in summer (Campbell, 2017; Fowler et al., 2015; Healy,  
35 2003; McKee, 1989). Therefore, it has been hypothesized that a warmer world may lower  
36 winter mortality in temperate climates (Langford & Bentham, 1995; Martens, 1998). In a large  
37 country like the USA, which possesses distinct climate regions, the seasonality of mortality  
38 may vary geographically, due to geographical variations in mortality, localized weather  
39 patterns, and regional differences in adaptation measures such as heating, air conditioning and  
40 healthcare (Davis, Knappenberger, Michaels, & Novicoff, 2004; Ferreira Braga, Zanobetti, &

Formatted: Font color: Text 1

Formatted: Font color: Text 1

Schwartz, 2001; Kalkstein, 2013; Medina-Ramón & Schwartz, 2007). The presence and extent of seasonal variation in mortality may also itself change over time, due to shifts in weather regimes, lifestyle, adaptation technologies, and healthcare (Bobb, Peng, Bell, & Dominici, 2014; Carson, Hajat, Armstrong, & Wilkinson, 2006; Seretakis, 1997; Sheridan, Kalkstein, & Kalkstein, 2009).

It is well-established that death rates vary throughout the year, and in temperate climates there tend to be more deaths in winter than in summer (Campbell, 2017; Fowler et al., 2015; Healy, 2003; McKee, 1989). It has therefore been hypothesized that a warmer world may lower winter mortality in temperate climates (Langford & Bentham, 1995; Martens, 1998). In a large country like the USA, which possesses distinct climate regions, the seasonality of mortality may vary geographically, due to geographical variations in mortality, localized weather patterns, and regional differences in adaptation measures such as heating, air conditioning and healthcare (Davis, Knappenberger, Michaels, & Novicoff, 2004; Ferreira Braga, Zanobetti, & Schwartz, 2001; Kalkstein, 2013; Medina-Ramón & Schwartz, 2007). The presence and extent of seasonal variation in mortality may also itself change over time (Bobb, Peng, Bell, & Dominici, 2014; Carson, Hajat, Armstrong, & Wilkinson, 2006; Seretakis, 1997; Sheridan, Kalkstein, & Kalkstein, 2009).

A thorough understanding of the long-term dynamics of seasonality of mortality, and its geographical and demographic patterns, is needed to identify at-risk groups, plan responses at the present time as well as under changing climate conditions. Although mortality seasonality is well-established, there is limited information on how seasonality, including the timing of minimum and maximum mortality, varies by local climate and how these features have changed over time, especially in relation to age group, sex and medical cause of death (Rau,

2004; Rau, Bohk-Ewald, Muszyńska, & Vaupel, 2018)(Rau, 2004; Rau, Bohk-Ewald, Muszyńska, & Vaupel, 2018).

In this paper, we comprehensively characterize the spatial and temporal patterns of all-cause and cause-specific mortality seasonality in the USA by sex and age group, through the application of wavelet analytical techniques, which have been used to study the dynamics of weather phenomena (Moy CM, Seltzer GO, Rodbell DT, 2002) and infectious diseases (Grenfell, Bjornstad, & Kappey, 2001), to over three decades of national mortality data. We also used centre of gravity analysis and circular statistics methods to understand the timing of mortality minimum and maximum where seasonality has been identified.

In this paper, we comprehensively characterize the spatial and temporal patterns of all-cause and cause-specific mortality seasonality in the USA by sex and age group, through the application of wavelet analytical techniques, to over three decades of national mortality data. Wavelets have been used to study the dynamics of weather phenomena (Moy, Seltzer, Rodbell, & Anderson, 2002) and infectious diseases (Grenfell, Bjørnstad, & Kappey, 2001). We also used centre of gravity analysis and circular statistics methods to understand the timing of mortality minimum and maximum. In addition, we identify how the percentage difference between death rates in maximum and minimum mortality months has changed over time.

## Results

Table 1 presents number of deaths by cause of death and sex. Deaths from cardiorespiratory diseases make up nearly half of all deaths (48.1%), with most deaths from cardiovascular diseases. Next highest during the study period were deaths from cancers (23.2%), followed by injuries (6.8%), with two thirds of those being from unintentional injuries.

All-cause mortality in males had a ~~statistically significant~~ 12-month seasonality in all age groups, except ~~in those aged~~ 35-44 years, for whom there was ~~statistically significant~~ periodicity at 6 months (Figure 2). In females, there was ~~significant~~ 12-month seasonality in all groups except 5-14 and 25-~~35~~34 years (~~p-values=0.21 and 0.25, respectively~~) (Figure 23). While seasonality persisted throughout the entire analysis period in older ages, it largely disappeared after late 1990s in children aged 0-4 years in both sexes and in women aged 15-24 years.

~~Mortality~~Deaths from all ~~four cause groups was~~ causes of death were seasonal ~~in older adults~~ (above ~~65 or 75 years of age~~ (Figure depending on cause, p-values<0.06) (Figures 2)-  
Seasonality in cancer deaths only appeared after 55 years of age, whereas deaths-11 and  
respective figure supplements), except for intentional injuries and substance use disorders.  
Deaths from cardiorespiratory ~~causes~~diseases, and within it respiratory infections, exhibited  
~~statistically significant~~ seasonality throughout the life-course. (~~p-values<0.06~~) except for males  
aged 5-24 years and females aged 15-24 years (~~p-values>0.11~~). In addition to older ages,  
~~injuries~~injury deaths were ~~also~~ seasonal from childhood through 44 years in women and  
through 64 years in men. (~~p-values<0.09~~). Unintentional injuries drove the seasonality of injury  
deaths for females, whereas both unintentional and intentional injuries were seasonal in males  
in most ages, with the exception of below 15 years and above 85 years when intentional injuries  
were not seasonal (Figure 8-figure supplement 1). Consistent seasonality in cancer deaths  
(Figures 3 and 4) only appeared after 55 years of age (~~p-values<0.05~~). No consistent seasonality  
was evident in substance use disorders (Figure 10-supplementary figure 5 and Figure 11-  
supplementary figure 5) or maternal conditions (Figure 11-supplementary figure 6).

Death

Centre of gravity analysis showed that death rates in men aged  $\geq 45$  years and women aged  $\geq 35$  years peaked in December, January and/or February and were lowest in June- to August, for all-cause mortality as well as for all non-injury and non-maternal causes of death with statistically significant seasonality (Figure 12 and respective figure supplements). Deaths from cardiorespiratory diseases, including injuries (Figure 3)-cardiovascular diseases, chronic respiratory diseases and respiratory infections, were also consistently highest in January and February and lowest in July and August across all ages, except for chronic respiratory diseases in ages 5-24 years where there are few deaths from this cause leading to unstable estimates (p-values for seasonality from wavelet analysis ranged from 0.35 to 0.48 for these ages). A similar temporal pattern was seen for all-cause and non-injury mortality in children younger than five years of age, whose all-cause death rate was highest in February and lowest in August. These months also represented maximum and minimum. In contrast, among males aged 5-34 years, all-cause mortality of children for non-injury causes. In contrast injury deaths in children, adolescents and young and middle-aged adults peaked in June/July and were lowest in December/January. Among older boys and young men, not only did injury mortality or July, as did deaths from injuries, which generally had a summer peak in in June/July, but all-cause mortality also. males and females below 45 years of age.

From 1980 to 2013<sup>36</sup>, the proportional (percent) difference in all-cause death rates between peak and minimum months declined little for people older than 45 years of age (non-significantly and by less than eight percentage points with p-values for declining trend  $> 0.1$ ) (Figure 413). In contrast, the difference between peak (summer) and minimum (winter) death rates declined significantly in younger ages, by over 25 percentage points in males aged 5-14 years and 15-24 years; (p-values  $< 0.01$ ), largely driven in the declining difference between summer and winter injury deaths. Under five years of age, percent seasonal difference in all-

cause death rates declined by ~~a statistically significant~~ 13 percentage points (95% CI 8 to 18p-value<0.01) for boys but only ~~a statistically non-significant~~ 5 percentage points (~~(p-value=0.12 to 2)~~) for girls. These declines in seasonality of child deaths were a net effect of declining winter-summer difference in cardiorespiratory diseases deaths and increasing summer-winter difference in injury deaths—, itself driven by increasing difference in non-intentional injuries (Figure 13-figure supplement 2). Within specific cardiorespiratory diseases in under-five children, percent difference declined for cardiorespiratory diseases, cardiovascular diseases, and chronic respiratory diseases while increasing for respiratory infections.

The subnational centre of gravity analysis showsed that all-cause mortality peaks and minima in different climate regions are consistent with the national ones (~~Figure 5~~Figures 14-17), indicating the seasonality is largely independent of geography. The relative homogeneity of the timing of maximum and minimum mortality contrasts with the large variation in seasonal temperatures among climate regions. For example, in men and women aged 65-74 years, all-cause mortality peaked in February in the Northeast and Southeast, even though the average temperatures for those regions were different by over 13 degrees Celsius (9.3 in the Southeast compared with -3.8 in the Northeast). Furthermore, above 45 years of age, there was little inter-region variation in the percent seasonal difference in all-cause mortality, despite the large variation in temperature difference between the peak and minimum months (Figure 6).~~The only cause of death with regional differences in seasonality was injuries in men aged 55-64 years and women aged 65-74 years. Injury death rates in these age-sex groups seemed to peak in January in the Northeast peak and in August in the~~ (Supplementary Figure 1).18).

#### Strengths and limitations

The strengths of our study are its innovative methods of characterizing seasonality of mortality dynamically over space and time, by age group and cause of death; using wavelet and centre of gravity analyses; using ERA-Interim data output to compare the association between seasonality of death rates and regional temperature. A limitation of our study is that we used broad causes of death so that we have sufficient number of deaths by age group, sex, year, climate region and cause of death. Different diseases and injuries may be differentially affected by environmental, behavioural and healthcare factors associated with season and hence differ in their seasonal behaviour. For example, suicides have been found to peak in early spring (Feinstein, 2002), and cardiovascular disease mortality may peak earlier in the winter than that from respiratory conditions (Mackenbach, Kunst, & Looman, 1992). Similarly, the seasonality of influenza, and how it has changed over time, may be different than that of other respiratory diseases due to disease-specific interventions (Simonsen et al., 2005). Further, we did not investigate seasonality of mortality by socioeconomic characteristics which may help with understanding its determinants and planning responses.

## Discussion

### Strengths and limitations

The strengths of our study are its innovative methods of characterizing seasonality of mortality dynamically over space and time, by age group and cause of death; using wavelet and centre of gravity analyses; using ERA-Interim data output to compare the association between seasonality of death rates and regional temperature. A limitation of our study is that we did not investigate seasonality of mortality by socioeconomic characteristics which may help with understanding its determinants and planning responses.



## Discussion

We used wavelet and centre of gravity analyses, which allowed ~~not only~~ systematically identifying and characterizing seasonality of total and cause-specific mortality in the USA, ~~but also examining how seasonality has changed over time. We identified distinct seasonal behaviours in relation to age and sex, including the higher summer mortality in young men (Feinstein, 2002; Rau et al., 2018).~~and examining how seasonality has changed over time. We ~~identified distinct seasonal patterns in relation to age and sex, including higher all-cause summer mortality in young men (Feinstein, 2002; Rau et al., 2018).~~ Importantly, we also showed that all-cause and cause-specific mortality seasonality is largely similar in terms of both timing and magnitude across diverse climatic regions with substantially different summer and winter temperatures, ~~with a notable exception of injuries in older ages.~~ Insights of this kind would not have been possible analysing data averaged over time or nationally, or fixed to pre-specified frequencies.

~~Prior studies have noted seasonality of mortality for all-cause mortality and for specific causes of death in the USA (Feinstein, 2002; Kalkstein, 2013; Rau, 2004; Rau et al., 2018; Rosenwaike, 1966; Seretakis, 1997). Few of these studies have done consistent national and subnational analyses, and none has done so over time, for a comprehensive set of age groups and causes of death, and in relation to regional temperature differences. Our results on strong seasonality of cardiorespiratory deaths and weak seasonality of cancer deaths, restricted to older ages, are broadly consistent with these studies (Feinstein, 2002; Rau et al., 2018; Rosenwaike, 1966; Seretakis, 1997), which had limited analysis on how seasonality changes over time and/or geography (Feinstein, 2002; Rau et al., 2018; Rosenwaike, 1966). Similarly, our results on seasonality of injury deaths are supported by a few prior studies (Feinstein, 2002; Rau et al., 2018; Rosenwaike, 1966), but our subnational analysis over three decades revealed~~

variations in when injury deaths peaked and in how seasonal differences in these deaths have changed over time which had not been reported before.

The observed geographical similarity in seasonal mortality variation in the USA, also seen in a study of 36 cities using deaths aggregated across age groups and over time (Kinney et al., 2015), contrasts from the pattern observed across Europe, where the difference between winter and summer mortality tends to be lower in the colder Nordic countries than in warmer southern European nations (Fowler et al., 2015; Healy, 2003; McKee, 1989). The absence of association between the magnitude of mortality seasonality and seasonal temperature difference indicates that different regions in the USA are similarly adapted to temperature seasonality, whereas Nordic countries may have better environmental (e.g., housing insulation and heating) and health system measures to counter the effects of cold winters than those in southern Europe.

The cause-specific analysis showed that the substantial decline in seasonal mortality differences in adolescents and young adults was related to the diminishing seasonality of injuries, especially from road traffic crashes, which are more likely to occur in the summer months (National Highway Traffic Safety Administration, 2005) and are more common in men. The weakening of seasonality in boys under five years of age was related to two phenomena: first, the seasonality of death from cardiorespiratory diseases declines, and second, the proportion of deaths during the perinatal period, which have limited seasonality, increased (MacDorman & Gregory, 2015).

Prior studies have noted seasonality of mortality for all-cause mortality and for specific causes of death in the USA (Feinstein, 2002; Kalkstein, 2013; Rau, 2004; Rau et al., 2018; Rosenwaike, 1966; Seretakis, 1997). Few of these studies have done consistent national and subnational analyses, and none has done so over time, for a comprehensive set of age groups

and causes of death, and in relation to regional temperature differences. Our results on strong seasonality of cardiorespiratory diseases deaths and weak seasonality of cancer deaths, restricted to older ages, are broadly consistent with these studies (Feinstein, 2002; Rau et al., 2018; Rosenwaike, 1966; Seretakis, 1997), which had limited analysis on how seasonality changes over time and geography (Feinstein, 2002; Rau et al., 2018; Rosenwaike, 1966). Similarly, our results on seasonality of injury deaths are supported by a few prior studies (Feinstein, 2002; Rau et al., 2018; Rosenwaike, 1966), but our subnational analysis over three decades revealed variations in when injury deaths peaked and in how seasonal differences in these deaths have changed over time in relation to age group which had not been reported before.

A study of 36 cities in the USA, aggregated across age groups and over time, also found that excess mortality was not associated with seasonal temperature range (Kinney et al., 2015). In contrast, a European study found that the difference between winter and summer mortality was lower in the colder Nordic countries than in warmer southern European nations (Healy, 2003; McKee, 1989)(the study's measure of temperature was mean annual temperature which differed from the temperature difference between maximum and minimum mortality used in our analysis although the two measures are correlated). The absence of variation in the magnitude of mortality seasonality indicates that different regions in the USA are similarly adapted to temperature seasonality, whereas Nordic countries may have better environmental (e.g., housing insulation and heating) and health system measures to counter the effects of cold winters than those in southern Europe. If the observed absence of association between the magnitude of mortality seasonality and seasonal temperature difference across the climate regions also persists over time, the changes in temperature as a result of global climate change are unlikely to affect the winter-summer mortality difference.

265

266 [The cause-specific analysis showed that the substantial decline in seasonal mortality](#)  
267 [differences in adolescents and young adults was related to the diminishing seasonality of](#)  
268 [\(unintentional\) injuries, especially from road traffic crashes, which are more likely to occur in](#)  
269 [the summer months \(National Highway Traffic Safety Administration, 2005\) and are more](#)  
270 [common in men. The weakening of seasonality in boys under five years of age was related to](#)  
271 [two phenomena: first, the seasonality of death from cardiorespiratory diseases declined, and](#)  
272 [second, the proportion of deaths from perinatal conditions, which exhibit limited seasonality](#)  
273 [\(Figure 10-figure supplement 4 and Figure 11-figure supplement 4\), increased \(MacDorman &](#)  
274 [Gregory, 2015\).](#)

275

276 In contrast to young and middle ages, mortality in older ages, where death rates are highest,  
277 maintained persistent seasonality over a period of three decades (we note that although the  
278 percent seasonal difference in mortality has remained largely unchanged in these ages, the  
279 absolute difference in death rates between the peak and minimum months has declined because  
280 total mortality has a declining long-term trend). This finding demonstrates the need for  
281 environmental and health service interventions targeted towards this group irrespective of  
282 geography and local climate. Examples of such interventions include enhancing the availability  
283 of both environmental and medical protective factors, such as better insulation of homes, winter  
284 heating provision and flu vaccinations, for the vulnerable older population ([Public Health](#)  
285 [England, 2017](#)).(Public Health England, 2017). Social interventions, including regular visits to  
286 the isolated elderly during peak mortality periods to ensure that they are optimally prepared for  
287 adverse conditions, and responsive and high-quality emergency care, are also important to  
288 protect this vulnerable group ([Healy, 2003; Lerchl, 1998; Public Health England, 2017](#)).(Healy,  
289 [2003; Lerchl, 1998; Public Health England, 2017](#)). Emergent new technologies, such as

290 always-connected hands-free communications devices with the outside world, in-house  
291 cameras, and personal sensors also provide an opportunity to enhance care for the older, more  
292 vulnerable groups in the population, especially in winter when the elderly have fewer social  
293 interactions ([Kimberly Miller, 2013](#)), ([Morris, 2013](#)). Such interventions are important today,  
294 and will remain so as the population ages and climate change increases the within- and  
295 between-season weather variability.

296

## 297 **Materials and methods**

### 298 *Data*

299 ~~We used data on all 77,771,264 deaths in the USA from 1980 to 2013 from the National Center~~  
300 ~~for Health Statistics (NCHS). Age, sex, state of residence, month of death, and underlying~~  
301 ~~cause of death were available for each record. Yearly population counts were available from~~  
302 ~~NCHS for 1990 to 2013 and from the US Census Bureau prior to 1990 (Ingram et al., 2003).~~  
303 ~~We calculated monthly population counts through linear interpolation, assigning each yearly~~  
304 ~~count to July. We also subdivided the national data geographically by climate regions used by~~  
305 ~~the National Oceanic and Atmospheric Administration (Figure 1) (Karl & Koss, 1984). The~~  
306 ~~underlying cause of death was coded according to the international classification of diseases~~  
307 ~~(ICD) system (9<sup>th</sup> revision of ICD from 1980 to 1998 and 10<sup>th</sup> revision of ICD thereafter).~~

308 We used data on all 85,854,176 deaths in the USA from 1980 to 2016 from the National Center  
309 for Health Statistics (NCHS). Age, sex, state of residence, month of death, and underlying  
310 cause of death were available for each record. The underlying cause of death was coded  
311 according to the international classification of diseases (ICD) system (9<sup>th</sup> revision of ICD from  
312 1980 to 1998 and 10<sup>th</sup> revision of ICD thereafter). Yearly population counts were available  
313 from NCHS for 1990 to 2016 and from the US Census Bureau prior to 1990 (Ingram et al.,

2003). We calculated monthly population counts through linear interpolation, assigning each yearly count to July.

We also subdivided the national data geographically into nine climate regions used by the National Oceanic and Atmospheric Administration (Figure 1 and Table 2) (Karl & Koss, 1984). On average, the Southeast and South are the hottest climate regions with average annual temperatures of 18.4°C and 18°C respectively; the South also possesses the highest average maximum monthly temperature (27.9°C in July). The lowest variation in temperature throughout the year is that of the Southeast (an average range of 17.5°C). The three coldest climate regions are West North Central, East North Central and the Northwest (7.8°C, 8.0°C, 8.1°C respectively). Mirroring the characteristics of the hottest climate regions, the largest variation in temperature throughout the year is that of the coldest region, West North Central (an average range of 30.5°C), which also has the lowest average minimum monthly temperature (-6.5°C in January). The other climate regions, Northeast, Southwest, and Central, possess similar average temperatures (11 to 13°C) and variation within the year of (23 to 26°C), with the Northeast being the most populous region in the United States (with 19.8% total population in 2016).

Data were divided by sex and age in the following 10 age groups: 0-4, 5-14, 25- 34, 35-44, 45-54, 55-64, 65-74, 75-84, 85+ years. We calculated monthly death rates for each age and sex group, both nationally and for sub-national climate regions. Death rate calculations accounted for varying length of months, by multiplying each month's death count by a factor that would make it equivalent to a 31-day month. For analysis of seasonality by cause of death, we mapped each ICD-9 and ICD-10 codes to the following four disease categories:

Formatted: Font color: Auto

- Cancers: ICD-9 140.0–239.9 and ICD-10 C00–D48
- Cardiorespiratory diseases: ICD-9 390.0–519.9 and ICD-10 I00–J99
- Injuries (external causes): ICD-9 800.0–999.9 and ICD-10 S00–Z99
- Other causes: ICD-9 and ICD-10 codes not in the above three categories

Cardiorespiratory diseases and cancers accounted for 56.4% and 21.2% of all deaths in the USA, respectively, in 1980, and 40.9% and 23.5%, respectively, in 2013. Deaths from cardiorespiratory diseases have been associated with cold and warm temperatures (Basu, 2009; Basu & Samet, 2002; Bennett, Blangiardo, Fecho, Elliott, & Ezzati, 2014; Braga, Zanobetti, & Schwartz, 2002; Gasparrini et al., 2015). Injuries, which accounted for 8% of all deaths in the USA in 1980 and 7.5% in 2013, may have seasonality that is distinct from so-called natural causes. We did not further divide other causes because the number of deaths could become too small to allow stable estimates when divided by age group, sex and climate region.

We obtained data on temperature from ERA-Interim, which combines predictions from a physical model with ground-based and satellite measurements (Dee et al., 2011). We used gridded four-times-daily estimates at a resolution of 80km to generate monthly population-weighted temperature by climate region throughout the analysis period.

#### *Statistical methods*

We used wavelet analysis to investigate seasonality, both nationally and sub-nationally, for each age-sex group. Wavelet analysis uncovers the presence, and frequency, of repeated maxima and minima in each age-sex-specific death rate time series. In brief, a Morlet wavelet, described in detail elsewhere (Cazelles et al., 2008), is equivalent to using a moving window on the death rate time series and analysing periodicity in each window using a short-form

Fourier transform, hence generating a dynamic spectral analysis, which allows measuring dynamic seasonal behaviour, in which the periodicity of death rates may disappear, emerge, or change over time. In addition to coefficients that measure the frequency of periodicity, wavelet analysis gives an indication of statistical significance of results compared with random fluctuations that can be represented with white (an independent random process) or red (autoregressive of order 1 process) noise. We used the R package WaveletComp (version 1.0) for the wavelet analysis. Before analysis, we logarithmically transformed death rates, detrended using a polynomial regression, and rescaled each all-cause mortality death rate time series so as to range between 1 and -1.

We identified age-sex groups whose wavelet power spectra differed from that of a white noise spectrum, which represents random fluctuations, at 5% significance level, for the entire study period (1980-2013). For age-sex groups which had statistically significant power spectra for 1980-2013 For analysis of seasonality by cause of death, we mapped each ICD-9 and ICD-10 codes to four main disease categories (Table 1) and to a number of subcategories which are presented in the Supplementary Note. Cardiorespiratory diseases and cancers accounted for 56.4% and 21.2% of all deaths in the USA, respectively, in 1980, and 40.3% and 22.4%, respectively, in 2016. Deaths from cardiorespiratory diseases have been associated with cold and warm temperatures (Basu, 2009; Basu & Samet, 2002; Bennett, Blangiardo, Fecht, Elliott, & Ezzati, 2014; Braga, Zanobetti, & Schwartz, 2002; Gasparrini et al., 2015). Injuries, which accounted for 8% of all deaths in the USA in 1980 and 7.3% in 2016, may have seasonality that is distinct from so-called natural causes. We did not further divide other causes because the number of deaths could become too small to allow stable estimates when divided by age group, sex and climate region.



We obtained data on temperature from ERA-Interim, which combines predictions from a physical model with ground-based and satellite measurements (Dee et al., 2011). We used gridded four-times-daily estimates at a resolution of 80km to generate monthly population-weighted temperature by climate region throughout the analysis period.

#### *Statistical methods*

We used wavelet analysis to investigate seasonality for each age-sex group. Wavelet analysis uncovers the presence, and frequency, of repeated maxima and minima in each age-sex-specific death rate time series (Hubbard, 1998; Torrence & Compo, 1998). In brief, a Morlet wavelet, described in detail elsewhere (Cazelles et al., 2008), is equivalent to using a moving window on the death rate time series and analysing periodicity in each window using a short-form Fourier transform, hence generating a dynamic spectral analysis, which allows measuring dynamic seasonal patterns, in which the periodicity of death rates may disappear, emerge, or change over time. In addition to coefficients that measure the frequency of periodicity, wavelet analysis estimates the probability of whether the data are different from the null situation of random fluctuations that can be represented with white (an independent random process) or red (autoregressive of order 1 process) noise. For each age-sex group, we calculated the p-values of the presence of 12-month seasonality for the comparison of wavelet power spectra of the entire study period (1980-2016) with 100 simulations against a white noise spectrum, which represents random fluctuations. We used the R package WaveletComp (version 1.0) for the wavelet analysis. Before analysis, we de-trended death rates using a polynomial regression, and rescaled each death rate time series so as to range between 1 and -1.

To identify the months of maximum and minimum death rates, we calculated the centre of gravity and the negative centre of gravity of monthly death rates. These parameters show when

in the year, on average, maximum and minimum death rates occur, respectively. For calculating centre of gravity, each month was calculated as a weighted average of months of deaths, with each month weighted by its death rate; for negative centre of gravity, was also calculated as a weighted average of months of deaths, but with each month was weighted by the difference between its death rate and the year's maximum death rate. In taking the weighted average, we allowed January (month 1) to neighbour December (month 12), a technique called circular statistics. December (month 12) to neighbour January (month 1), representing each month by an angle subtended from 12 equally-spaced points around a unit circle. Using a technique called circular statistics, a mean ( $\bar{\theta}$ ) of the angles ( $\theta_1, \theta_2, \theta_3 \dots, \theta_n$ ) representing the deaths (with  $n$  the total number of deaths in an age-sex group for a particular cause of death) is found using the relation below:

$$\bar{\theta} = \arg \left\{ \sum_{j=1}^n \exp(i\theta_j) \right\},$$

where  $\arg$  denotes the complex number argument and  $\theta_j$  denotes the month of death in angular form for a particular death  $j$ . The outcome of this calculation is then converted back into a month value (Fisher, 1995). Along with each circular mean, a 95% confidence interval (CI) was calculated by using 1000 bootstrap samples. The R package CircStats (version 0.2.4) was used for this purpose analysis.

For each age-sex group and cause of death, and for each year, we calculated the percent difference in death rates between the maximum and minimum mortality months. We fitted a linear regression to the time series of seasonal differences from 1980 to 2016, and used a Poisson model the fitted trend line to estimate how much the percentage difference in death rates between the maximum and minimum mortality months for each year, and its standard error which accounts for population size. We then fitted a linear regression to the time series

438 of seasonal differences for each age and sex group, weighting each had changed from 1980 to  
439 2016. We weighted seasonal difference by the inverse of the square of its standard error. We  
440 calculated, which was calculated using a Poisson model to take population size of each age-  
441 sex group through time into account. This method gives us a p-value for the change in the fitted  
442 values from 1980 to 2013, reported as percentage point difference, as a quantitative seasonal  
443 difference per year, which we used to calculate the seasonal difference at the start (1980) and  
444 end (2016) of the period of study. Our method of analysing seasonal differences avoids  
445 assuming that any specific month or group of months represent highest and lowest number of  
446 deaths for a particular cause of death, which is the approach taken by the traditional measure  
447 of how the seasonality of death rates has changed over time. Excess Winter Deaths. It also  
448 allows the maximum and minimum mortality months to vary by age group, sex and cause of  
449 death.

450

#### 451 **Acknowledgments**

452 Robbie Parks is supported by a Wellcome Trust ISSF Studentship. Work on the US mortality  
453 data is supported by a grant from US Environmental Protection Agency.

454

#### 455 **Author contributions**

456 All authors contributed to study concept, analytical approach, and interpretation of results. RP,  
457 KF and ME collated and organised mortality files. RP performed the analysis, with input from  
458 JB. RP and ME wrote the first draft of the paper; other authors contributed to revising and  
459 finalising the paper.

460

#### 461 **Competing financial interests**

462 The authors declare no competing financial interests.

Formatted: Font:Not Bold

## References

- Basu, R. (2009). High ambient temperature and mortality: a review of epidemiologic studies from 2001 to 2008. *Environmental Health*, 8(4), 40. *A Global Access Science Source*. <https://doi.org/10.1186/1476-069X-8-40>
- Basu, R., & Samet, J. M. (2002). Relation between elevated ambient temperature and mortality: A review of the epidemiologic evidence. *Epidemiologic Reviews*. <https://doi.org/10.1093/epirev/mxf007>
- Bennett, J. E., Blangiardo, M., Fecht, D., Elliott, P., & Ezzati, M. (2014). Vulnerability to the mortality effects of warm temperature in the districts of England and Wales. *Nature Climate Change*, 4(4), 269–273. <https://doi.org/10.1038/nclimate2123>
- Bobb, J. F., Peng, R. D., Bell, M. L., & Dominici, F. (2014). Heat-related mortality and adaptation to heat in the United States. *Environmental Health Perspectives*, 122(8), 811–816. <https://doi.org/10.1289/ehp.1307392>
- Braga, A. L. F., Zanobetti, A., & Schwartz, J. (2002). The effect of weather on respiratory and cardiovascular deaths in 12 U.S. cities. *Environmental Health Perspectives*, 110(9), 859–863. <https://doi.org/10.1289/ehp.02110859>
- Campbell, A. (2017). Excess winter mortality in England and Wales: 2016 to 2017 (provisional) and 2015 to 2016 (final). *Statistical Bulletin, Office for National Statistics*.
- Carson, C., Hajat, S., Armstrong, B., & Wilkinson, P. (2006). Declining vulnerability to temperature-related mortality in London over the 20th century. *American Journal of Epidemiology*, 164(1), 77–84. <https://doi.org/10.1093/aje/kwj147>
- Cazelles, B., Chavez, M., Berteaux, D., Ménard, F., Vik, J. O., Jenouvrier, S., & Stenseth, N. C. (2008). Wavelet analysis of ecological time series. *Oecologia*. <https://doi.org/10.1007/s00442-008-0993-2>
- Davis, R. E., Knappenberger, P. C., Michaels, P. J., & Novicoff, W. M. (2004). Seasonality of climate-human mortality relationships in US cities and impacts of climate change. *Climate Research*, 26(1), 61–76. Retrieved from internal-pdf://32.0.35.211/paper.pdf
- Dee, D. P., Uppala, S. M., Simmons, A. J., Berrisford, P., Poli, P., Kobayashi, S., ... Vitart, F. (2011). The ERA-Interim reanalysis: configuration and performance of the data assimilation system. *Quarterly Journal of the Royal Meteorological Society*, 137(656), 553–597. <https://doi.org/10.1002/qj.828>
- Feinstein, C. A. (2002). Seasonality of deaths in the U.S. by age and cause. *Demographic Research*, 6, 469–486. <https://doi.org/10.4054/DemRes.2002.6.17>
- Ferreira Braga, A. L., Zanobetti, A., & Schwartz, J. (2001). The time course of weather-related deaths. *Epidemiology*, 12(6), 662–667. <https://doi.org/10.1097/00001648-200111000-00014>
- Fisher, N. I. (1995). *Statistical analysis of circular data*. Cambridge University Press.
- Fowler, T., Southgate, R. J., Waite, T., Harrell, R., Kovats, S., Bone, A., ... Murray, V. (2015). Excess winter deaths in Europe: A multi-country descriptive analysis. *European Journal of Public Health*, 25(2), 339–345. <https://doi.org/10.1093/eurpub/cku073>
- Gasparrini, A., Guo, Y., Hashizume, M., Lavigne, E., Zanobetti, A., Schwartz, J., ... Armstrong, B. (2015). Mortality risk attributable to high and low ambient temperature: A multicountry observational study. *The Lancet*, 386(9991), 369–375. [https://doi.org/10.1016/S0140-6736\(14\)62114-0](https://doi.org/10.1016/S0140-6736(14)62114-0)
- Grenfell, B. T., Bjørnstad, O. N., & Kappey, J. (2001). Travelling waves and spatial hierarchies in measles epidemics. *Nature*, 414(6865), 716–723. <https://doi.org/10.1038/414716a>
- Healy, J. D. (2003). Excess winter mortality in Europe: A cross country analysis identifying key risk factors. *Journal of Epidemiology and Community Health*, 57(10), 784–789. <https://doi.org/10.1136/jech.57.10.784>

Formatted: Justified

Field Code Changed

Formatted: Justified

Hubbard, B. B. (1998). *The world according to wavelets: the story of a mathematical technique in the making*. A K Peters/CRC Press.

Ingram, D. D., Parker, J. D., Schenker, N., Weed, J. A., Hamilton, B., Arias, E., & Madans, J. H. (2003). United States Census 2000 population with bridged race categories. *Vital and Health Statistics. Series 2, Data Evaluation and Methods Research*, (135), 1–55. Retrieved from internal-pdf://103.99.132.94/paper.pdf

Kalkstein, A. J. (2013). Regional Similarities in Seasonal Mortality across the United States: An Examination of 28 Metropolitan Statistical Areas. *PLoS ONE*, 8(5). <https://doi.org/10.1371/journal.pone.0063971>

Karl, T. R., & Koss, W. J. (1984). Regional and national monthly, seasonal, and annual temperature weighted by area, 1895-1983.

Kimberly Miller, A. A. (2013). Smart-Home Technologies to Assist Older People to Live Well at Home. *Journal of Aging Science*, 1(1). <https://doi.org/10.4172/2329-8847.1000101>

Kinney, P. L., Schwartz, J., Pascal, M., Petkova, E., Tertre, A. Le, Medina, S., & Vautard, R. (2015). Winter season mortality: Will climate warming bring benefits? *Environmental Research Letters*, 10(6). <https://doi.org/10.1088/1748-9326/10/6/064016>

Langford, I. H., & Bentham, G. (1995). The potential effects of climate change on winter mortality in England and Wales. *Int J Biometeorol*, 38(3), 141–147. Retrieved from internal-pdf://189.27.88.183/art%253A10.1007%252F01208491.pdf

Lerchl, A. (1998). Changes in the seasonality of mortality in Germany from 1946 to 1995: the role of temperature. *International Journal of Biometeorology*, 42(2), 84–88. <https://doi.org/10.1007/s004840050089>

MacDorman, M. F., & Gregory, E. (2015). Fetal and Perinatal Mortality: United States, 2013. *National Vital Statistics Reports*, 64(8), 1–24.

Mackenbach, J. P., Kunst, A. E., & Looman, C. W. N. (1992). Seasonal variation in mortality in The Netherlands. *Journal of Epidemiology and Community Health*, 46(3), 261–265. <https://doi.org/10.1136/jech.46.3.261>

Martens, W. J. (1998). Climate change, thermal stress and mortality changes. *Soc Sci Med*, 46(3), 331–344. Retrieved from internal-pdf://57.13.130.132/1-s2.0-S0277953697001627-main.pdf

McKee, C. M. (1989). Deaths in winter: Can Britain learn from Europe? *European Journal of Epidemiology*, 5(2), 178–182. <https://doi.org/10.1007/BF00156826>

Medina-Ramón, M., & Schwartz, J. (2007). Temperature, temperature extremes, and mortality: A study of acclimatisation and effect modification in 50 US cities. *Occupational and Environmental Medicine*, 64(12), 827–833. <https://doi.org/10.1136/oem.2007.033175>

Morris, M. E. (2013). Smart-Home Technologies to Assist Older People to Live Well at Home. *Journal of Aging Science*, 01(01). <https://doi.org/10.4172/2329-8847.1000101>

Moy, C. M., Seltzer, G. O., Rodbell, D. T., & Anderson, D. M. (2002). Variability of El Niño/Southern Oscillation activity at millennial timescales during the Holocene epoch. *Nature*, 420(November), 6912, 162–165. <https://doi.org/10.1038/nature01194>

National Highway Traffic Safety Administration. (2005). Trend and Pattern Analysis of Highway Crash Fatality By Month and Day. *National Center for Statistics and Analysis (NCHS)*, (March).

Public Health England. (2017). The Cold Weather Plan for England. *Public Health England*, (October).

Rau, R. (2004). Seasonality in Human Mortality. A Demographic Approach. *Wirtschafts- Und Sozialwissenschaftlichen Fakultät, PhD*, 361. <https://doi.org/10.1007/978-3-540-44902-7>

Rau, R., Bohk-Ewald, C., Muszyńska, M. M., & Vaupel, J. W. (2018). *Visualizing Mortality*

Formatted: Justified

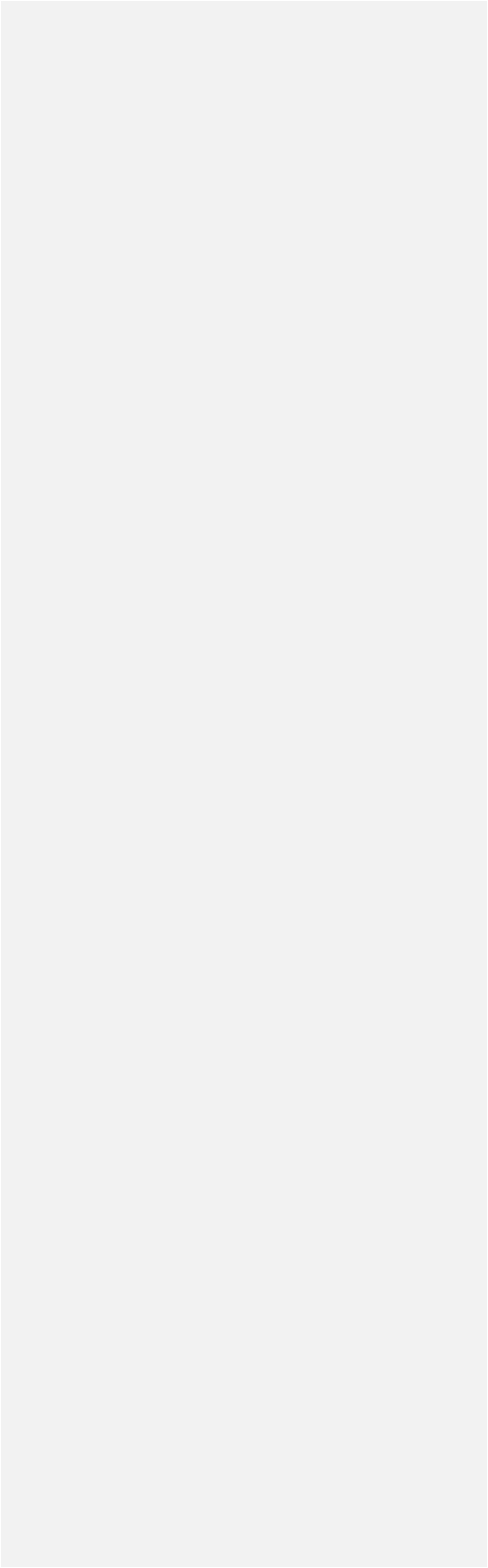
Formatted: Justified

Formatted: Justified

Formatted: Justified

563 *Dynamics in the Lexis Diagram*. <https://doi.org/10.1007/978-3-319-64820-0>  
 564 Rosenwaike, I. (1966). Seasonal Variation of Deaths in the United States, 1951–1960. *Journal*  
 565 *of the American Statistical Association*, 61(315), 706–719.  
 566 <https://doi.org/10.1080/01621459.1966.10480899>  
 567 Seretakis, D. (1997). Changing Seasonality of Mortality From Coronary Heart Disease. *JAMA:*  
 568 *The Journal of the American Medical Association*, 278(12), 1012.  
 569 <https://doi.org/10.1001/jama.1997.03550120072036>  
 570 Sheridan, S. C., Kalkstein, A. J., & Kalkstein, L. S. (2009). Trends in heat-related mortality in  
 571 the United States, 1975–2004. *Natural Hazards*, 50(1), 145–160.  
 572 <https://doi.org/10.1007/s11069-008-9327-2>  
 573 Simonsen, L., Reichert, T. A., Viboud, C., Blackwelder, W. C., Taylor, R. J., & Miller, M. A.  
 574 (2005). Impact of influenza vaccination on seasonal mortality in the US elderly  
 575 population. *Archives of Internal Medicine*, 165(3), 265–272.  
 576 <https://doi.org/10.1001/archinte.165.3.265>  
 577 Torrence, C., & Compo, G. P. (1998). A Practical Guide to Wavelet Analysis. *Bulletin of the*  
 578 *American Meteorological Society*. [https://doi.org/10.1175/1520-](https://doi.org/10.1175/1520-0477(1998)079<0061:APGTWA>2.0.CO;2)  
 579 [0477\(1998\)079<0061:APGTWA>2.0.CO;2](https://doi.org/10.1175/1520-0477(1998)079<0061:APGTWA>2.0.CO;2)  
 580

Formatted: Justified



582 **Figure 2:** Wavelet power spectra for national time series of all-cause ~~and cause-specific~~ death  
583 rates for 1980-2013<sup>36</sup>, by age group ~~and cause of death~~ for (A) males ~~and (B) females~~. Wavelet  
584 power values increase from blue to red, ~~with white contour lines indicating~~. The shaded regions  
585 ~~at the 5% significance level against a white noise spectrum (left and right edge of each box~~  
586 ~~indicate the same~~ cone of influence, where spectral analysis is less robust. P-values for the  
587 ~~presence of 12-month seasonality are to the right of each figure at the 12-month line.~~  
588



589 [Figure 3: Wavelet power spectra for national time series of all-cause death rates for 1980-](#)  
590 [2016, by age groups would remain significant if significance had been measured against a group](#)  
591 [for females. Wavelet power values increase from blue to red noise spectrum\).](#) The shaded  
592 regions at the left and right edge of each box indicate the cone of influence, where spectral  
593 analysis is less robust.

594 [P-values for the presence of 12-month seasonality are to the right of each figure at the 12-](#)  
595 [month line.](#)  
596

597 **Figure 4:** [Wavelet power spectra for national time series of cancer death rates for 1980-2016,](#)  
598 [by age group for males. Wavelet power values increase from blue to red. The shaded regions](#)  
599 [at the left and right edge of each box indicate the cone of influence, where spectral analysis is](#)  
600 [less robust. P-values for the presence of 12-month seasonality are to the right of each figure at](#)  
601 [the 12-month line.](#)  
602

603 **Figure 5:** Wavelet power spectra for national time series of cancer death rates for 1980-2016,  
604 by age group for females. Wavelet power values increase from blue to red. The shaded regions  
605 at the left and right edge of each box indicate the cone of influence, where spectral analysis is  
606 less robust. P-values for the presence of 12-month seasonality are to the right of each figure at  
607 the 12-month line.

**Figure 6:** Wavelet power spectra for national time series of cardiorespiratory disease death rates for 1980-2016, by age group for males. Wavelet power values increase from blue to red. The shaded regions at the left and right edge of each box indicate the cone of influence, where spectral analysis is less robust. P-values for the presence of 12-month seasonality are to the right of each figure at the 12-month line.

**Figure 6-figure supplement 1:** Wavelet power spectra for national time series of cardiovascular disease death rates for 1980-2016, by age group for males. Wavelet power values increase from blue to red. The shaded regions at the left and right edge of each box indicate the cone of influence, where spectral analysis is less robust. P-values for the presence of 12-month seasonality are to the right of each figure at the 12-month line.

**Figure 6-figure supplement 2:** Wavelet power spectra for national time series of chronic respiratory disease death rates for 1980-2016, by age group for males. Wavelet power values increase from blue to red. The shaded regions at the left and right edge of each box indicate the cone of influence, where spectral analysis is less robust. P-values for the presence of 12-month seasonality are to the right of each figure at the 12-month line.

**Figure 6-figure supplement 3:** Wavelet power spectra for national time series of respiratory infection death rates for 1980-2016, by age group for males. Wavelet power values increase from blue to red. The shaded regions at the left and right edge of each box indicate the cone of influence, where spectral analysis is less robust. P-values for the presence of 12-month seasonality are to the right of each figure at the 12-month line.

**Figure 7:** Wavelet power spectra for national time series of cardiorespiratory disease death rates for 1980-2016, by age group for females. Wavelet power values increase from blue to red. The shaded regions at the left and right edge of each box indicate the cone of influence, where spectral analysis is less robust. P-values for the presence of 12-month seasonality are to the right of each figure at the 12-month line.

**Figure 7-figure supplement 1:** Wavelet power spectra for national time series of cardiovascular disease death rates for 1980-2016, by age group for females. Wavelet power values increase from blue to red. The shaded regions at the left and right edge of each box indicate the cone of influence, where spectral analysis is less robust. P-values for the presence of 12-month seasonality are to the right of each figure at the 12-month line.

**Figure 7-figure supplement 2:** Wavelet power spectra for national time series of chronic respiratory disease death rates for 1980-2016, by age group for females. Wavelet power values increase from blue to red. The shaded regions at the left and right edge of each box indicate the cone of influence, where spectral analysis is less robust. P-values for the presence of 12-month seasonality are to the right of each figure at the 12-month line.

**Figure 7-figure supplement 3:** Wavelet power spectra for national time series of respiratory infection death rates for 1980-2016, by age group for females. Wavelet power values increase from blue to red. The shaded regions at the left and right edge of each box indicate the cone of influence, where spectral analysis is less robust. P-values for the presence of 12-month seasonality are to the right of each figure at the 12-month line.

658 **Figure 8:** Wavelet power spectra for national time series of injury death rates for 1980-2016,  
659 by age group for males. Wavelet power values increase from blue to red. The shaded regions  
660 at the left and right edge of each box indicate the cone of influence, where spectral analysis is  
661 less robust. P-values for the presence of 12-month seasonality are to the right of each figure at  
662 the 12-month line.

663  
664 **Figure 8-figure supplement 1:** Wavelet power spectra for national time series of intentional  
665 injury death rates for 1980-2016, by age group for males. Wavelet power values increase from  
666 blue to red. The shaded regions at the left and right edge of each box indicate the cone of  
667 influence, where spectral analysis is less robust. P-values for the presence of 12-month  
668 seasonality are to the right of each figure at the 12-month line.

669  
670 **Figure 8-figure supplement 2:** Wavelet power spectra for national time series of unintentional  
671 injury death rates for 1980-2016, by age group for males. Wavelet power values increase from  
672 blue to red. The shaded regions at the left and right edge of each box indicate the cone of  
673 influence, where spectral analysis is less robust. P-values for the presence of 12-month  
674 seasonality are to the right of each figure at the 12-month line.

675  
676

677 **Figure 9:** Wavelet power spectra for national time series of injury death rates for 1980-2016,  
678 by age group for females. Wavelet power values increase from blue to red. The shaded regions  
679 at the left and right edge of each box indicate the cone of influence, where spectral analysis is  
680 less robust. P-values for the presence of 12-month seasonality are to the right of each figure at  
681 the 12-month line.

682  
683 **Figure 9-figure supplement 1:** Wavelet power spectra for national time series of intentional  
684 injury death rates for 1980-2016, by age group for females. Wavelet power values increase  
685 from blue to red. The shaded regions at the left and right edge of each box indicate the cone of  
686 influence, where spectral analysis is less robust. P-values for the presence of 12-month  
687 seasonality are to the right of each figure at the 12-month line.

688  
689 **Figure 9-figure supplement 2:** Wavelet power spectra for national time series of unintentional  
690 injury death rates for 1980-2016, by age group for females. Wavelet power values increase  
691 from blue to red. The shaded regions at the left and right edge of each box indicate the cone of  
692 influence, where spectral analysis is less robust. P-values for the presence of 12-month  
693 seasonality are to the right of each figure at the 12-month line.

694  
695



**Figure 10:** Wavelet power spectra for national time series of death rates from causes other than cancers, cardiorespiratory diseases and injuries for 1980-2016, by age group for males. Wavelet power values increase from blue to red. The shaded regions at the left and right edge of each box indicate the cone of influence, where spectral analysis is less robust. P-values for the presence of 12-month seasonality are to the right of each figure at the 12-month line.

**Figure 10-figure supplement 1:** Wavelet power spectra for national time series of endocrine disorder death rates for 1980-2016, by age group for males. Wavelet power values increase from blue to red. The shaded regions at the left and right edge of each box indicate the cone of influence, where spectral analysis is less robust. P-values for the presence of 12-month seasonality are to the right of each figure at the 12-month line.

**Figure 10-figure supplement 2:** Wavelet power spectra for national time series of genitourinary disease death rates for 1980-2016, by age group for males. Wavelet power values increase from blue to red. The shaded regions at the left and right edge of each box indicate the cone of influence, where spectral analysis is less robust. P-values for the presence of 12-month seasonality are to the right of each figure at the 12-month line.

**Figure 10-figure supplement 3:** Wavelet power spectra for national time series of neuropsychiatric disorder death rates for 1980-2016, by age group for males. Wavelet power values increase from blue to red. The shaded regions at the left and right edge of each box indicate the cone of influence, where spectral analysis is less robust. P-values for the presence of 12-month seasonality are to the right of each figure at the 12-month line.

**Figure 10-figure supplement 4:** Wavelet power spectra for national time series of perinatal condition death rates for 1980-2016, by age group for males. Wavelet power values increase from blue to red. The shaded regions at the left and right edge of each box indicate the cone of influence, where spectral analysis is less robust. P-values for the presence of 12-month seasonality are to the right of each figure at the 12-month line.

**Figure 10-figure supplement 5:** Wavelet power spectra for national time series of substance use disorder death rates for 1980-2016, by age group for males. Wavelet power values increase from blue to red. The shaded regions at the left and right edge of each box indicate the cone of influence, where spectral analysis is less robust. P-values for the presence of 12-month seasonality are to the right of each figure at the 12-month line.

**Figure 11:** Wavelet power spectra for national time series of death rates from causes other than cancers, cardiorespiratory diseases and injuries for 1980-2016, by age group for females. Wavelet power values increase from blue to red. The shaded regions at the left and right edge of each box indicate the cone of influence, where spectral analysis is less robust. P-values for the presence of 12-month seasonality are to the right of each figure at the 12-month line.

**Figure 11-figure supplement 1:** Wavelet power spectra for national time series of endocrine disorder death rates for 1980-2016, by age group for females. Wavelet power values increase from blue to red. The shaded regions at the left and right edge of each box indicate the cone of influence, where spectral analysis is less robust. P-values for the presence of 12-month seasonality are to the right of each figure at the 12-month line.

**Figure 11-figure supplement 2:** Wavelet power spectra for national time series of genitourinary disease death rates for 1980-2016, by age group for females. Wavelet power values increase from blue to red. The shaded regions at the left and right edge of each box indicate the cone of influence, where spectral analysis is less robust. P-values for the presence of 12-month seasonality are to the right of each figure at the 12-month line.

**Figure 11-figure supplement 3:** Wavelet power spectra for national time series of neuropsychiatric disorder death rates for 1980-2016, by age group for females. Wavelet power values increase from blue to red. The shaded regions at the left and right edge of each box indicate the cone of influence, where spectral analysis is less robust. P-values for the presence of 12-month seasonality are to the right of each figure at the 12-month line.

**Figure 11-figure supplement 4:** Wavelet power spectra for national time series of perinatal condition death rates for 1980-2016, by age group for females. Wavelet power values increase from blue to red. The shaded regions at the left and right edge of each box indicate the cone of influence, where spectral analysis is less robust. P-values for the presence of 12-month seasonality are to the right of each figure at the 12-month line.

**Figure 11-figure supplement 5:** Wavelet power spectra for national time series of substance use disorder death rates for 1980-2016, by age group for females. Wavelet power values increase from blue to red. The shaded regions at the left and right edge of each box indicate the cone of influence, where spectral analysis is less robust. P-values for the presence of 12-month seasonality are to the right of each figure at the 12-month line.

**Figure 11-figure supplement 6:** Wavelet power spectra for national time series of maternal condition death rates for 1980-2016, by age group for females. Wavelet power values increase from blue to red. The shaded regions at the left and right edge of each box indicate the cone of influence, where spectral analysis is less robust. P-values for the presence of 12-month seasonality are to the right of each figure at the 12-month line.

776 **Figure 12:** Mean timing of ~~national~~ maximum and minimum all-cause and cause-specific  
777 mortality ~~at the national level~~, by sex and age group for 1980-2013~~6~~. Red arrows indicate the  
778 month of maximum mortality, and green arrows that of minimum mortality. The size of the  
779 arrow is inversely proportional to its respective ~~95% confidence interval~~. ~~Only age-sex groups~~  
780 ~~with statistically significant 12-month seasonality are included.~~

781 [variance.](#)

782

783 **Figure 412-figure supplement 1:** [Mean timing of maximum and minimum mortality for](#)  
784 [specific cardiorespiratory diseases at the national level, by sex and age group for 1980-2016.](#)

785 [Red arrows indicate the month of maximum mortality, and green arrows that of minimum](#)  
786 [mortality. The size of the arrow is inversely proportional to its respective variance.](#)

787

788 **Figure 12-figure supplement 2:** [Mean timing of maximum and minimum mortality for](#)  
789 [specific injuries at the national level, by sex and age group for 1980-2016. Red arrows indicate](#)  
790 [the month of maximum mortality, and green arrows that of minimum mortality. The size of the](#)  
791 [arrow is inversely proportional to its respective variance.](#)

792

793 **Figure 12-figure supplement 3:** [Mean timing of maximum and minimum mortality for the](#)  
794 [cluster of causes other than cancers, cardiorespiratory diseases and injuries at the national level,](#)  
795 [by sex and age group for 1980-2016. Red arrows indicate the month of maximum mortality,](#)  
796 [and green arrows that of minimum mortality. The size of the arrow is inversely proportional to](#)  
797 [its respective variance.](#)

798 **Figure 13:** National percent difference in death rates between the maximum and minimum  
799 mortality months ~~in 2013~~ for all-cause and cause-specific mortality in 2016 versus 1980 ~~by sex~~  
800 ~~and age group. Only age-sex groups with statistically significant 12-month seasonality are~~  
801 ~~included. Age-sex groups with a statistically significant change at the 5% level are highlighted~~  
802 ~~with a bold pink outline.~~

803 [, by sex and age group.](#)

804

805 **Figure 513-figure supplement 1:** [National percent difference in death rates between the](#)  
806 [maximum and minimum mortality months for specific cardiorespiratory diseases in 2016](#)  
807 [versus 1980, by sex and age group.](#)

808

809 **Figure 13-figure supplement 2:** [National percent difference in death rates between the](#)  
810 [maximum and minimum mortality months for specific injuries in 2016 versus 1980, by sex and](#)  
811 [age group.](#)

812

813 **Figure 13-figure supplement 3:** [National percent difference in death rates between the](#)  
814 [maximum and minimum mortality months for the cluster of causes other than cancers,](#)  
815 [cardiorespiratory diseases and injuries in 2016 versus 1980, by sex and age group.](#)



816 **Figure 14:** Mean timing of ~~(A)-maximum and (B)-minimum~~ all-cause mortality for 1980-2016,  
817 by climate region, ~~sex~~ and age group for ~~1980-2013. Only age-sex groups with significant 12-~~  
818 ~~month seasonality males. Average temperatures (in the national analysis~~degrees Celsius) are  
819 included in white for the corresponding month of maximum and minimum mortality for each  
820 climate region.

821 **Figure 15:** Mean timing of minimum all-cause mortality for 1980-2016, by climate region and  
822 age group for males. Average temperatures (in degrees Celsius) are included in white for the  
823 corresponding month of maximum and minimum mortality for each climate region.

824 **Figure 16:** Mean timing of maximum all-cause mortality for 1980-2016, by climate region and  
825 age group for females. Average temperatures (in degrees Celsius) are included in white for the  
826 corresponding month of maximum and minimum mortality for each climate region.

827 [Figure 17: Mean timing of minimum all-cause mortality for 1980-2016, by climate region and](#)  
828 [age group for females](#). Average temperatures (in degrees Celsius) are included in white for the  
829 corresponding month of maximum and minimum mortality for each climate region. [See](#)  
830 [Supplementary Figure 1 for results by cause of death](#).

831 **Figure 618:** The relationship between percent difference in [all-cause](#) death rates and  
832 temperature difference between months with maximum and minimum mortality across climate  
833 regions, by sex and age group in 2013. ~~Only age-sex groups with significant 12-month~~  
834 ~~seasonality in the national analysis are included.~~2016.▲

**Formatted:** Font:Not Bold, Font color: Text 1

835 **Supplementary Figure 1:** Mean timing of (A) maximum and (B) minimum cause-specific  
836 mortality, by climate region, sex and age group for 1980-2013. Only age-sex groups with  
837 significant 12-month seasonality in the national analysis are included. Average temperatures  
838 (in degrees Celsius) are included in white for the corresponding month of maximum and  
839 mortality for each climate region. **Table 1:** Number of deaths, by cause of death and sex from  
840 1980 to 2016.

<b>Cause</b>		<b>Male</b>	<b>Female</b>	<b>Total</b>
All cause		43,558,203	42,295,973	85,854,176
-	Cancers	10,481,582	9,476,530	19,958,112
-	Cardiorespiratory diseases	20,168,049	21,109,525	41,277,574
-	Cardiovascular diseases	16,238,344	17,210,556	33,448,900
-	Chronic respiratory diseases	2,791,652	2,595,950	5,387,602
-	Respiratory infections	1,138,053	1,303,019	2,441,072
-	Injuries	4,034,876	1,768,170	5,803,046
-	Unintentional	2,489,142	1,348,187	3,837,329
-	Intentional	1,545,734	419,983	1,965,717
-	Other causes	8,873,696	9,941,748	18,815,444

841

**Table 2:** Characteristics of climate regions of the USA.

<u>Climate region</u>	<u>Constituent states</u>	<u>Population (2016)</u>	<u>Mean annual temperature (1980-2016) (°C)</u>
<u>Central</u>	<u>Illinois, Indiana, Kentucky, Missouri, Ohio, Tennessee, West Virginia</u>	<u>50,191,326</u>	<u>11.6</u>
<u>East North Central</u>	<u>Iowa, Michigan, Minnesota, Wisconsin</u>	<u>24,418,738</u>	<u>8</u>
<u>Northeast</u>	<u>Connecticut, Delaware, Maine, Maryland, Massachusetts, New Hampshire, New Jersey, New York, Pennsylvania, Rhode Island, Vermont</u>	<u>64,046,741</u>	<u>10.6</u>
<u>Northwest</u>	<u>Alaska, Idaho, Oregon, Washington</u>	<u>13,811,810</u>	<u>8.2</u>
<u>South</u>	<u>Arkansas, Kansas, Louisiana, Mississippi, Oklahoma, Texas</u>	<u>45,388,414</u>	<u>18</u>
<u>Southeast</u>	<u>Alabama, Florida, Georgia, North Carolina, South Carolina, Virginia</u>	<u>59,356,072</u>	<u>18.4</u>
<u>Southwest</u>	<u>Arizona, Colorado, New Mexico, Utah</u>	<u>17,613,981</u>	<u>13.6</u>
<u>West</u>	<u>California, Hawaii, Nevada</u>	<u>43,708,574</u>	<u>16.6</u>
<u>West North Central</u>	<u>Montana, Nebraska, North Dakota, South Dakota, Wyoming</u>	<u>5,168,753</u>	<u>7.6</u>